The Impact of Diverse Preprocessing Pipelines on Brain Functional Connectivity

Eva Výtvarová[*†], Jan Fousek[*†], Marek Bartoň[†], Radek Mareček[†], Martin Gajdoš[†], Martin Lamoš[†],
Marie Nováková[†], Tomáš Slavíček[†], Igor Peterlik[‡§] and Michal Mikl[†]

[*]Faculty of Informatics, Masaryk University, Brno, Czech Republic

Email: eva.vytvarova@mail.muni.cz

[†]Multimodal and Functional Neuroimaging Research Group, CEITEC, Masaryk University, Brno, Czech Republic

[‡]Institute of Computer Science, Masaryk University, Brno, Czech Republic

[§]Inria, France

Abstract—**Brain functional connectivity measured by functional magnetic resonance imaging was shown to be influenced by preprocessing procedures. We aim to describe this influence separately for different preprocessing factors and in 20 different most used preprocessing pipelines. We evaluate the effects of slice-timing correction and physiological noise filtering by RETROICOR, diverse levels of motion correction, and white matter, cerebrospinal fluid, and global signal filtering. With usage of three datasets, we show the impact on global metrics of resting-state functional brain networks and their reliability. We show negative effect of RETROICOR on reliability of metrics and disrupting effect of global signal regression on network topology. We do not support the use of slice-timing correction because it does not significantly influence any of the measured features. We also show that the selected types of preprocessing may affect averaged node strength, normalized clustering coefficient, normalized characteristic path length and modularity.**

I. INTRODUCTION

Functional magnetic resonance imaging (fMRI) provides unique possibilities to study brain activity at rest and during a task at reasonably good spatial and temporal scales when compared to other modalities for functional brain imaging. Statistical dependence between diverse brain regions is referred to as a functional connectivity. It has been shown that functional connectivity at rest is strongly influenced by disease [1], [2] or cognitive state [3].

The functional connectivity pattern in brain can be seen as a network composed of nodes—regions of interest (ROIs)—and edges, i.e., connections between pairs of nodes representing statistical relationship (e.g. similarity between time series of measured signals) [1]. The network topology and importance of nodes within network can be quantified by metrics (also called measures) such as characteristic path length or clustering coefficient. A reproducibility of network metrics was studied in [4], workflow for brain functional connectivity analysis is proposed in [5]. The comparisons of networks of different sizes [6] and analytical approaches [7], together with recommendations of how to treat negative correlations [8] and how to threshold the results [9], form a background for brain connectivity analyses.

However, one has to deal with a complex preprocessing procedure prior to the actual data analysis. Many preprocessing
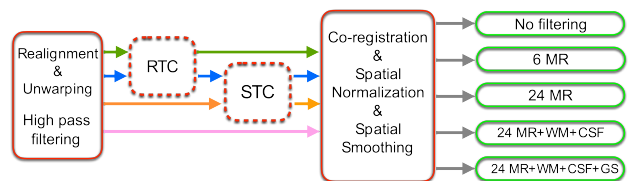
Fig. 1. Schema of 20 evaluated variants of preprocessing pipelines.

methods have been proposed in the last years targeting reliability in individuals [10], [11], temporal filtering at frequency bands [11], slice-timing correction (STC) [12], motion artifacts [13], [14], physiological noise correction—cardiac and respiratory-cycle effects [15], [16]—or specifics like global signal filtering [3], cerebrospinal fluid (CSF) and white matter (WM) regression [3]. These studies, however, mostly target only a specific effect of preprocessing of the data. Follow-up studies such as [17], [18], [19], [20], [21] evaluated specific preprocessing steps and their impact of diverse features of functional connectivity.

We aim to quantify a complex influence of preprocessing pipeline on two aspects of functional connectivity – its topology and reliability in time. Therefore, we examine different preprocessing pipelines covering usage of STC, RETROICOR [15] for cardiac and breathing filtering, high pass filtering, movement correction, WM, CSF and global signal (GS) filtering. Our study is inspired by the consensual pipeline for structural brain networks evaluating different parcellation atlases [22] and is a direct extension to [20], [18], [21].

II. METHODS

A. Data preprocessing

The fMRI data was preprocessed using SPM8 [23]. The whole pipeline with variants evaluated in this study is illustrated in Fig. 1. The first step consisted of realignment and unwarp, optional high pass filtering with cutoff at 128 s, optional RETROICOR correction (**RTC**), optional slice-timing correction (**STC**)—the middle slice was chosen as the referential one, co-registration of the structural scan to the mean functional image, spatial normalization (with segmentation) of the structural scan to the Montreal Neurological Institute

template, spatial normalization and spatial smoothing of the functional data, Gaussian kernel of FWHM = 8 mm.

Second step of preprocessing is the noise suppression. We filter the data by regression approach with general linear model $Y = X * b + e$, where Y is BOLD signal time-series from preprocessed data, X is design matrix containing models of noise as individual regressors, b stands for parameters describing linear combination of regressors, and e stands for residual time-series, that is the BOLD signal time-series after filtering (after the effects of noise are removed from the data). We evaluated separate effects of 4 preprocessing factors, all possible combinations of these factors and their variants (creating 48 distinct preprocessing pipelines), from which we picked and analyzed in more detail 5 different settings of X, as denoted in scheme in Fig.1, that are the most frequent combinations of preprocessing steps used for subsequent functional connectivity analyses. The preprocessing factors are:

high pass filtering (hpf):
- no
- cutoff 128 s,

movement regression:
- no
- 6MR (6 movement regressors (MR; 3 translations and 3 rotations) estimated during `realign` procedure in SPM8),
- 24MR (extended set of 24 MR (3 translations, 3 rotations, their time-differences and all of them squared) [13]),

WM and CFS regression (NV):
- no
- only CSF (6 CSF signals)
- only WM (4 WM signals)
- CSF + WM (6 CSF, 4 WM signals),

global signal regression:
- no
- global signal calculated using SPM8 (function `spm_global`).

B. Functional connectivity

Functional connectivity for every measurement in our datasets was assessed between each pair of specific brain regions. We used Automated Anatomical Labeling (AAL) atlas for parcellation of brain into specific regions [24]. 80 AAL regions fulfilled the criterion of minimal coverage of valid data (50%, voxelwise) among all subjects and thus were used for subsequent analysis. First principal component was used as a representative signal from all valid voxels in particular AAL region [18] resulting in 80 representative time-series for each subject corresponding to the selected 80 AAL regions. These time-series were detrended (removing mean and linear drift) and were used for calculation of Pearson's correlation coefficients yielding 80x80 correlation matrix. Further, the Fisher's Z-transformation was applied to the matrix.

This procedure was repeated for all filtering combinations resulting in 48 correlation matrices for each of 4 combinations of correction (RTC, STC, RTC+STC, simple proc.) for each

subject. Moreover, we calculated correlation matrices for the first half of BOLD signal time-series and for the second half, to be able to estimate a split-half reliability.

C. Measures of functional connectivity

The effects on network topology (networks defined by correlation matrices) were analyzed using global level network analytical measures – normalized clustering coefficient, normalized characteristic path length, modularity, and averaged node strength. The *Brain Connectivity Toolbox* was used [25] and normalization was assured by values computed for 100 null models. The metrics were assessed for weighted networks.

Network measures were further computed for networks of the first and second halves of the AAL ROI time-series. The split-half reliability was computed on network level as an intra-class correlation coefficient (ICC) [26]. This metric was used in previous resting-state fMRI studies [10], [11].

Generalized linear mixed model implemented in the SPSS Statistics software was used to quantify the impact of preprocessing pipelines on studied measures, using a significance threshold $p < 0.05$. The model included two factors—correction and filtering—and their interference. Follow-up post-hoc tests of individual differences were interpreted on $p < 0.05$ with Bonferroni correction for multiple comparisons.

III. DATA AND RESULTS

A. Subjects and data acquisition

Three datasets were acquired for this study: Null300, NullVob, Prisma. None of the subjects scanned to perform this study reported any previous neurological or psychiatric disorders. All subjects have given their written informed consent and the study was approved by the local ethics board. The datasets specifications are following:

Null300: 1.5 T Siemens Symphony scanner, resting state fMRI, 15 minutes, time of scan repetition (TR) = 3 s, 300 scans; voxel size 3.45x3.45x3.5 mm, 52 subjects,

NullVob: 1.5 T Siemens Symphony scanner, resting state fMRI, 7 minutes, TR = 1.66 s, 256 scans; voxel size 3.9x3.9x6 mm, 52 subjects (the same subjects as in the Null300 dataset),

Prisma: 3T Siemens Prisma scanner, resting state fMRI, 15 minutes, TR = 0.65 s, 1370 scans, voxel size 3x3x3 mm; 19 subjects (completely different set of subjects than in the previous datasets).

Further, high-resolution anatomical T1-weighted images were acquired using the MP-RAGE sequence. The ECG and respiration signal data were recorded simultaneously during functional measurement using the MR compatible EEG/ExG system (Brain Products, Germany) with a 5 kHz sampling rate and a resolution of $10\mu V$.

B. Results

In weighted networks, considering separate effects of factors on network measures, we observed an extreme influence of global signal regression on all studied metrics. The high pass filtering also caused statistically significant changes in all

TABLE I
SEPARATE EFFECTS OF PREPROCESSING FACTORS ON NETWORK PROPERTIES. MEANS AND STANDARD ERRORS ARE SHOWN.

dataset:		Null300		NullVob		Prisma	
metric:		normalized clustering coefficient					
hpf	no	1.260 (0.075)	$p < 0.001$	1.273 (0.078)	$p < 0.05$	1.224 (1.800)	$p < 0.001$
	yes	1.272 (0.075)		1.269 (0.078)		1.272 (1.800)	
MR	no	1.260 (0.075)	$p(noMR, 6MR) < 0.001$	1.270 (0.078)		1.239 (1.800)	
	6MR	1.268 (0.075)	$p(noMR, 24MR) < 0.001$	1.274 (0.078)	$p > 0.05$	1.253 (1.800)	$p > 0.05$
	24MR	1.268 (0.075)	$p(6MR, 24MR) > 0.05$	1.270 (0.078)		1.252 (1.800)	
NV	no	1.266 (0.075)		1.263 (0.078)	$p(no, CSF) < 0.001$	1.252 (1.800)	
	CSF	1.264 (0.075)	$p > 0.05$	1.278 (0.078)	$p(CSF, WM) < 0.001$ $p(no, CSF|WM) < 0.001$	1.249 (1.800)	$p > 0.05$
	WM	1.268 (0.075)		1.266 (0.078)	$p(no, WM) < 0.05$	1.245 (1.800)	
	CSF+WM	1.266 (0.075)		1.279 (0.078)	$p(CSF, CSF|WM) > 0.05$	1.246 (1.800)	
GS	no	1.039 (0.075)	$p < 0.001$	1.035 (0.078)	$p < 0.001$	1.028 (1.800)	$p < 0.001$
	yes	1.493 (0.075)		1.508 (0.078)		1.468 (1.800)	
metric:		normalized characteristic path length					
hpf	no	1.316 (0.061)	$p < 0.001$	1.319 (0.503)	$p < 0.001$	1.350 (0.113)	$p < 0.001$
	yes	1.330 (0.061)		1.314 (0.503)		1.380 (0.113)	
MR	no	1.319 (0.061)	$p(noMR, 6MR) < 0.001$	1.319 (0.503)	$p(noMR, 6MR) > 0.05$	1.356 (0.113)	
	6MR	1.327 (0.061)	$p(noMR, 24MR) < 0.05$	1.321 (0.503)	$p(noMR, 24MR) < 0.001$	1.368 (0.113)	$p > 0.05$
	24MR	1.322 (0.061)	$p(6MR, 24MR) < 0.001$	1.310 (0.503)	$p(6MR, 24MR) < 0.001$	1.370 (0.113)	
NV	no	1.314 (0.061)	$p(no, CSF) < 0.001$ $p(no, WM) < 0.001$	1.302 (0.503)		1.363 (0.113)	
	CSF	1.327 (0.061)	$p(no, CSF|WM) < 0.001$	1.323 (0.503)	$p < 0.001$	1.365 (0.113)	$p > 0.05$
	WM	1.320 (0.061)	$p(CSF, WM) < 0.001$ $p(WM, CSF|WM) < 0.001$	1.313 (0.503)		1.362 (0.113)	
	CSF+WM	1.329 (0.061)	$p(CSF, CSF|WM) > 0.05$	1.330 (0.503)		1.368 (0.113)	
GS	yes	1.174 (0.061)	$p < 0.001$	1.141 (0.503)	$p < 0.001$	1.173 (0.113)	$p < 0.001$
	no	1.471 (0.061)		1.493 (0.503)		1.556 (0.113)	
metric:		averaged node strength					
hpf	no	21.806 (4.717)	$p < 0.001$	22.662 (4.960)	$p < 0.001$	26.112 (5.064)	$p < 0.001$
	yes	19.929 (4.717)		22.272 (4.960)		24.190 (5.064)	
MR	no	21.709 (4.718)		23.363 (4.961)		27.392 (5.066)	
	6MR	20.953 (4.718)	$p < 0.001$	22.412 (4.961)	$p < 0.001$	24.442 (5.066)	$p < 0.001$
	24MR	19.939 (4.718)		21.624 (4.961)		23.619 (5.066)	
NV	no	23.151 (4.718)		25.314 (4.961)		26.772 (5.068)	$p(no, CSF) < 0.001$
	CSF	19.953 (4.718)	$p < 0.001$	20.880 (4.961)	$p < 0.001$	24.511 (5.068)	$p(no, WM) < 0.001$ $p(no, CSF|WM) < 0.001$
	WM	21.391 (4.718)		23.672 (4.961)		25.609 (5.068)	$p(WM, CSF|WM) < 0.001$
	CSF+WM	18.973 (4.718)		20.000 (4.961)		23.712 (5.068)	$p(CSF, WM) < 0.05$ $p(CSF, CSF|WM) < 0.05$
GS	no	34.561 (4.717)	$p < 0.001$	37.756 (4.960)	$p < 0.001$	42.444 (5.064)	$p < 0.001$
	yes	7.173 (4.717)		7.177 (4.960)		7.858 (5.064)	
metric:		modularity coefficient					
hpf	no	0.248 (0.388)	$p < 0.001$	0.249 (0.032)	$p < 0.05$	0.226 (0.008)	$p < 0.001$
	yes	0.259 (0.388)		0.248 (0.032)		0.241 (0.008)	
MR	no	0.249 (0.388)	$p(noMR, 6MR) < 0.001$	0.247 (0.032)	$p(noMR, 6MR) < 0.001$	0.227 (0.008)	$p(noMR, 6MR) < 0.001$
	6MR	0.255 (0.388)	$p(noMR, 24MR) < 0.001$	0.250 (0.032)	$p(noMR, 24MR) < 0.05$	0.237 (0.008)	$p(noMR, 24MR) < 0.001$
	24MR	0.257 (0.388)	$p(6MR, 24MR) < 0.05$	0.249 (0.032)	$p(6MR, 24MR) > 0.05$	0.237 (0.008)	$p(6MR, 24MR) > 0.05$
NV	no	0.246 (0.388)		0.237 (0.032)		0.231 (0.008)	
	CSF	0.256 (0.388)	$p < 0.001$	0.255 (0.032)	$p < 0.001$	0.235 (0.008)	$p > 0.05$
	WM	0.252 (0.388)		0.243 (0.032)		0.232 (0.008)	
	CSF+WM	0.261 (0.388)		0.259 (0.032)		0.236 (0.008)	
GS	no	0.131 (0.388)	$p < 0.001$	0.188 (0.032)	$p < 0.001$	0.090 (0.008)	$p < 0.001$
	yes	0.376 (0.388)		0.379 (0.032)		0.377 (0.008)	

metrics, however, these changes are small (up till 10% in averaged node strength and till 5% in higher order metrics). Similar effect was caused by movement regression, especially on averaged node strength (the more sophisticated movement regression, the lower averaged node strength values). The averaged node strength was also decreased by filtering of WM, CSF (and GS). The white matter and cerebrospinal fluid filtering increase normalized characteristic path length and modularity coefficient (affected only minimally up till 10% of a value with no filtering). This is even more pronounced when correcting for global signal. The results for normalized characteristic path length are in detail captured by Figure 2a.

These results were similar across all three datasets, although in Prisma dataset the metrics are less influenced by preprocessing factors. The details are captured by Table I.

The adaptation of RTC significantly increases averaged node strength, especially in preprocessing combinations with less sophisticated movement regression, as visualized in Fig. 2b. This was found in all datasets. The metrics computed on Null300 dataset are overall more influenced by RTC than other dataset, we also measured decreased normalized characteristic path length and modularity (Fig. 2c) in this dataset.

The STC was not applied in the Prisma dataset because of short TR. In this dataset, we measured increased variance of characteristic path length values in RTC variant.

We found no consistent effect of slice-timing correction on studied features. The effects became significant only when combined with RTC.

Considering reliability computed by ICC, we observed worse results when adapting RTC across all metrics and datasets (for illustration see Fig. 3a). Slice-timing correction and high pass filtering slightly improve reliability of characteristic path length and modularity (Fig. 3b). As well as
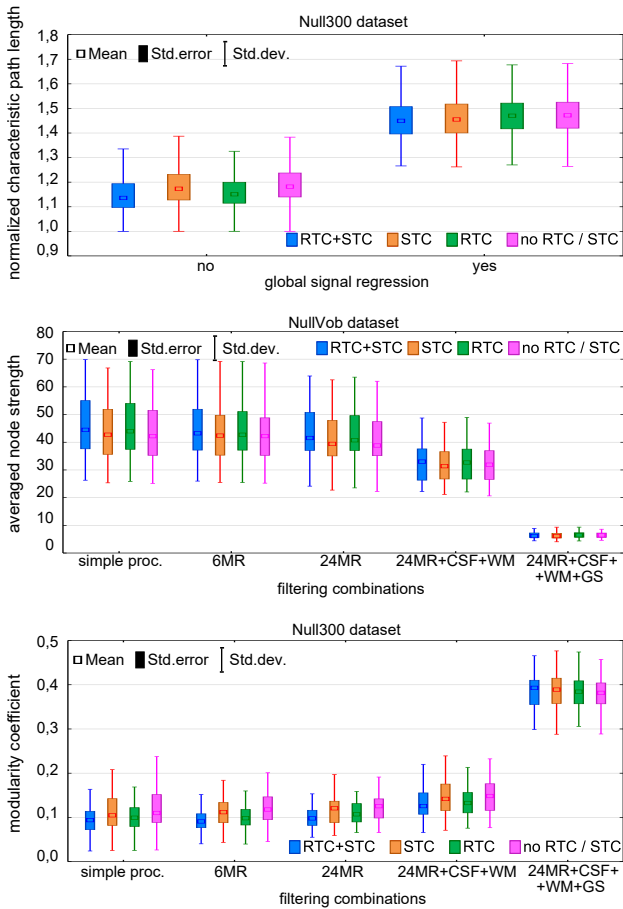
Fig. 2. Effect of a) global signal regression on normalized characteristic path length (Null300 dataset), RTC and STC on b) averaged node strength (NullVob dataset), c) modularity coefficient (Null300 dataset) of the most typical filtering combinations.

Fig. 3. Effect of a) RTC and STC on reliability of averaged node strength of the most typical filtering combinations, b) RTC, STC and high pass filtering on reliability of modularity coefficient (both Null300 dataset), c) global signal regression on reliability of studied metrics (NullVob dataset).

in differences in global metrics values between preprocessing pipelines, the global signal regression influences, specifically increases, the reliability of all studied metrics across all datasets. This effect is shown in Fig. 3c.

IV. DISCUSSION AND CONCLUSIONS

The evaluation of effects of preprocessing pipelines on network structure revealed significant shift towards more regular network structure (higher normalized clustering coefficient and normalized characteristic path length) with more prominent modular structure (increased modularity coefficient) when filtering WM, CSF (and GS) signals and when regressing out the movement. This was observed in Null300 and NullVob datasets. The Prisma dataset seems to give more stable results suggesting the network topology is less influenced by preprocessing. The filtering also caused decreases in averaged node strength in all datasets which can be interpreted as decreases in connectivity.

We want to emphasize extreme effect of global signal regression on all metrics across all datasets—drastic decreases of connectivity combined with increases of clustering and path length lead to more regular network with low connectivity

strength. We observed the GS influence in all datasets. Partially overlapping conclusions were drawn in [18], however, other metrics were studied in this paper.

High pass filtering was also found to affect network topology and connectivity strength, but even though its influence is statistically significant, the changes in metrics values are lacking practical significance. However, care has to be taken in meta-analyses where these slight differences can lead to diverse trends.

The normalized characteristic path length was also influenced by RTC and interactive effect of RTC / RTC+STC and filtration—lower values when using RETROICOR. The same trends—higher level of filtering and use of RETROICOR increase values of a metric—were present in modularity coefficient describing the ability of network to form functionally similar clusters. Taking averaged node strength into account, the significant effects of RTC and filtering steps as well as their combinations were measured. Specifically, the more filtering steps included, the lower the values, as concluded also by [18], while RETROICOR kept values higher. These findings relate to Null300 dataset. In other studied datasets the RTC has effect only on averaged node strength of networks with low level of additional filtering.

As to describe the differences between networks constructed from the first and second halves of time-series, we computed intra-class correlation coefficient and found impact of RTC on all studied metrics consistently across datasets. We argue that lower ICC values of metrics with preprocessing including RETROICOR could be caused by time-series dynamics getting more pronounced by breathing and cardiac artifacts correction.

Slice-timing correction and high pass filtering slightly increase reliability of modularity coefficient and normalized characteristic path length. As on the level of network metrics values, the global signal regression influences the reliability of studied metrics. We believe the increased reliability when correcting for GS is caused by disturbed network topology and compromised neural characteristics of the time-series that underly studied networks.

To conclude, we observed negative effect of RETROICOR on split-half reliability, however, future studies have to be conducted to explain the origin of this effect. We did not find convincing evidence for using slice-timing correction. In agreement with previous studies [18], [19], [20], [21] and following our results, we suggest to not use the filtering of global signal in the stage of data preprocessing. To further investigate the impact of preprocessing pipeline on functional connectivity, we will test the features for group discriminability, which is crucial when evaluating potential markers of a disease. Our results further alert to careful choice of studies entering meta-analyses since seemingly miniscule differences in preprocessing pipelines can lead to very different results. Similar diversity of results based on processing pipeline was reported by [17] for analysis of task-related fMRI data. We strongly recommend especially to not combine studies with different approaches concerning global signal filtering. The same applies to complex studies where network analysis is one of the studied aspects.

REFERENCES

[1] E. Bullmore and O. Sporns, "Complex brain networks: graph theoretical analysis of structural and functional systems." *Nature reviews. Neuroscience*, vol. 10, no. 3, pp. 186–198, 2009.

[2] Y. Liu, M. Liang, Y. Zhou, Y. He, Y. Hao, M. Song, C. Yu, H. Liu, Z. Liu, and T. Jiang, "Disrupted small-world networks in schizophrenia," *Brain*, vol. 131, no. 4, pp. 945–961, 2008.

[3] W. Shirer, S. Ryali, E. Rykhlevskaia, V. Menon, and M. Greicius, "Decoding subject-driven cognitive states with whole-brain connectivity patterns," *Cerebral cortex*, vol. 22, no. 1, pp. 158–165, 2012.

[4] L. Deuker, E. T. Bullmore, M. Smith, S. Christensen, P. J. Nathan, B. Rockstroh, and D. S. Bassett, "Reproducibility of graph metrics of human brain functional networks," *NeuroImage*, vol. 47, no. 4, pp. 1460–1468, 2009.

[5] M. Kaiser, "A tutorial in connectome analysis: topological and spatial features of brain networks." *NeuroImage*, vol. 57, no. 3, pp. 892–907, aug 2011.

[6] B. C. M. van Wijk, C. J. Stam, and A. Daffertshofer, "Comparing brain networks of different size and connectivity density using graph theory," *PLoS ONE*, vol. 5, no. 10, 2010.

[7] A. Zalesky, L. Cocchi, A. Fornito, M. M. Murray, and E. Bullmore, "Connectivity differences in brain networks," *NeuroImage*, vol. 60, no. 2, pp. 1055–1062, 2012.

[8] X. J. Chai, A. N. Castañán, D. Öngür, and S. Whitfield-Gabrieli, "Anti-correlations in resting state networks without global signal regression," *NeuroImage*, vol. 59, pp. 1420–1428, 2012.

[9] M. Drakesmith, K. Caeyenberghs, A. Dutt, G. Lewis, A. David, and D. Jones, "Overcoming the effects of false positives and threshold bias in graph theoretical analyses of neuroimaging data," *NeuroImage*, 2015.

[10] Z. Shehzad, A. C. Kelly, P. T. Reiss, D. G. Gee, K. Gotimer, L. Q. Uddin, S. H. Lee, D. S. Margulies, A. K. Roy, B. B. Biswal *et al.*, "The resting brain: unconstrained yet reliable," *Cerebral cortex*, vol. 19, no. 10, pp. 2209–2229, 2009.

[11] C. C. Guo, F. Kurth, J. Zhou, E. A. Mayer, S. B. Eickhoff, J. H. Kramer, and W. W. Seeley, "One-year test–retest reliability of intrinsic connectivity network fMRI in older adults," *NeuroImage*, vol. 61, no. 4, pp. 1471–1483, 2012.

[12] R. Sladky, K. J. Friston, J. Tröstl, R. Cunnington, E. Moser, and C. Windischberger, "Slice-timing effects and their correction in functional MRI," *NeuroImage*, vol. 58, no. 2, pp. 588–594, 2011.

[13] K. J. Friston, S. Williams, R. Howard, R. S. Frackowiak, and R. Turner, "Movement-related effects in fMRI time-series," *Magnetic resonance in medicine*, vol. 35, no. 3, pp. 346–355, 1996.

[14] J. D. Power, B. L. Schlaggar, and S. E. Petersen, "Recent progress and outstanding issues in motion correction in resting state fMRI," *NeuroImage*, vol. 105, pp. 536–551, 2015.

[15] G. H. Glover, T.-Q. Li, and D. Ress, "Image-based method for retrospective correction of physiological motion effects in fMRI: RETROICOR," *Magnetic Resonance in Medicine*, vol. 44, no. 1, pp. 162–167, 2000.

[16] C. Chang and G. H. Glover, "Effects of model-based physiological noise correction on default mode network anti-correlations and correlations," *NeuroImage*, vol. 47, no. 4, pp. 1448–1459, 2009.

[17] J. Carp, "On the plurality of (methodological) worlds: Estimating the analytic flexibility of fmri experiments," *Frontiers in Neuroscience*, vol. 6, no. OCT, pp. 1–13, 2012.

[18] U. Braun, M. M. Plichta, C. Esslinger, C. Sauer, L. Haddad, O. Grimm, D. Mier, S. Mohnke, A. Heinz, S. Erk *et al.*, "Test-retest reliability of resting-state connectivity network characteristics using fMRI and graph theoretical measures," *NeuroImage*, vol. 59, no. 2, pp. 1404–1412, 2012.

[19] C.-G. Yan, R. C. Craddock, Y. He, and M. P. Milham, "Addressing head motion dependencies for small-world topologies in functional connectomics," *Frontiers in Human Neuroscience*, vol. 7, no. 910, 2013.

[20] W. R. Shirer, H. Jiang, C. M. Price, B. Ng, and M. D. Greicius, "Optimization of rs-fMRI Pre-processing for Enhanced Signal-Noise Separation, Test-Retest Reliability, and Group Discrimination," *NeuroImage*, 2015.

[21] N. K. Aurich, J. O. A. Filho, A. M. M. da Silva, and A. R. Franco, "Evaluating the reliability of different preprocessing steps to estimate graph theoretical measures in resting state fMRI data," *Frontiers in Neuroscience*, vol. 9, no. FEB, pp. 1–10, 2015.

[22] C. S. Parker, F. Deligianni, M. J. Cardoso, P. Daga, M. Modat, M. Dayan, C. A. Clark, S. Ourselin, and J. D. Clayden, "Consensus between Pipelines in Structural Brain Networks," *PLoS ONE*, vol. 9, no. 10, 2014.

[23] K. Friston, J. Ashburner, S. Kiebel, T. Nichols, and W. Penny, Eds., *Statistical Parametric Mapping: The Analysis of Functional Brain Images*. Academic Press, 2007.

[24] N. Tzourio-Mazoyer, B. Landeau, D. Papathanassiou, F. Crivello, O. Etard, N. Delcroix, B. Mazoyer, and M. Joliot, "Automated anatomical labeling of activations in SPM using a macroscopic anatomical parcellation of the MNI MRI single-subject brain." *NeuroImage*, vol. 15, no. 1, pp. 273–89, jan 2002.

[25] M. Rubinov and O. Sporns, "Complex network measures of brain connectivity: Uses and interpretations," *NeuroImage*, vol. 52, no. 3, pp. 1059–1069, 2010.

[26] P. E. Shrout and J. L. Fleiss, "Intraclass correlations: uses in assessing rater reliability." *Psychological bulletin*, vol. 86, no. 2, p. 420, 1979.